Journal of Atmospheric and Solar-Terrestrial Physics 73 (2011) 1228–1241

Contents lists available at ScienceDirect

Journal of Atmospheric and Solar-Terrestrial Physics

journal homepage: www.elsevier.com/locate/jastp

Multipoint ICME encounters: Pre-STEREO and STEREO observations

E.K.J. Kilpua [a,*], L.K. Jian [b], Y. Li [c], J.G. Luhmann [c], C.T. Russell [b]

[a] Department of Physics, Division of Geophysics and Astronomy, P.O. Box 64, University of Helsinki, Finland
[b] Institute of Geophysics and Planetary Physics, UCLA, Los Angeles, CA, USA
[c] Space Sciences Laboratory, University of California, Berkeley, CA, USA

ARTICLE INFO

Article history:
Received 4 March 2010
Received in revised form
20 October 2010
Accepted 21 October 2010
Available online 20 November 2010

Keywords:
Interplanetary coronal mass ejections
Magnetic cloud
Solar wind
Multipoint observations

ABSTRACT

The knowledge of the global properties of interplanetary coronal mass ejections (ICMEs) is of great interest for heliospheric research and space weather forecasting. Due to the large dimensions of ICMEs and the lack of systematic multipoint measurements the true three-dimensional configuration of ICMEs is still poorly understood. The launch of the STEREO twin observatory in October 2006 opened important new opportunities for ICME research. One of the scientific goals of the STEREO mission is to study the large-scale structure of ICMEs. In this paper we review the multi-spacecraft ICME observations conducted before the STEREO era and discuss the ICME properties that were identified at least by one of the STEREO spacecraft and those at the Lagrangian point L1 (Wind/ACE) from April 2007 through March 2008. The multi-spacecraft observations emphasize that ICMEs cannot be explained in terms of a simple flux rope model. The characteristics of ICMEs and the structure of the solar wind in which they were embedded varied significantly from event to event. The observations show that ICMEs can have cross-sectional shapes from almost circular to significantly distended. In the ecliptic plane ICMEs may span at least up to 40° in longitude, consistent with the angular span of the average CME close to the Sun. However, the association between the ICME observations at different spacecraft is not straightforward as significant differences were observed even when the spacecraft were separated by only a few degrees in longitude. In addition, multipoint observations confirm that the identification of the flux rope structure is modified by the spacecraft crossing distance from the center of the ICME. We show examples of the events where one spacecraft crosses the central flux rope, but the other spacecraft traverses the ICME close to the edge where the flux rope structure is no longer obvious.

© 2010 Elsevier Ltd. All rights reserved.

1. Introduction

Coronal mass ejections (CMEs) are huge magnetized plasma clouds that are hurled from the Sun into the interplanetary space. For more than 30 years CMEs have been detected remotely near the Sun and in situ in the interplanetary medium by various spacecraft. Near the Sun, CMEs span from only few degrees all the way to 360° around the occulting disk of the coronagraph (St. Cyr et al., 2000). The angular extent and appearance of a CME in coronagraph images depend not only on its actual size, but also on the location of the source at the solar disk and the complicated process of the Thomson scattering of photospheric light from the CME plasma (Cremades and Bothmer, 2004; Vourlidas and Howard, 2006). CMEs that originate close to the solar limb typically extend about 50° and this width is maintained as CMEs propagate away from the Sun (St. Cyr et al., 2000; Yashiro et al., 2004; Gopalswamy, 2006). CMEs propagate out into the heliosphere and when observed in situ in the interplanetary medium they are referred as interplanetary CMEs (ICMEs). ICMEs are distinguished from the normal solar wind by characteristic plasma, magnetic field and particle signatures (e.g., Gosling, 1990; Neugebauer and Goldstein, 1997; Richardson and Cane, 2004a; Zurbuchen and Richardson, 2006). At the orbit of the Earth, ICMEs have radial diameters on average about 0.4 AU including the shock and the sheath region if they exists (Jian et al., 2006) and they can span up to several tens of degrees in longitude.

Consequences of ICMEs are far-reaching in the heliosphere and thus, the knowledge of the three-dimensional structure of ICMEs is of key importance for solar-terrestrial research. Gosling et al. (1992) estimated that near the orbit of the Earth ICMEs comprise 15% of the solar wind at solar maximum while at larger heliospheric distances the contribution of ICMEs can be even higher than 40% (Wang and Richardson, 2004). Due to the intense magnetic fields and organized directional changes of the magnetic field, ICMEs often produce intense magnetic storms in the Earth's magnetosphere (e.g., Webb et al., 2000; Richardson et al., 2001; Huttunen et al., 2005). In addition, the knowledge of the global ICME geometry is essential when estimating the magnetic flux and helicity removed by CMEs from the Sun (e.g., Dasso et al., 2005).

The large-scale structure of an ICME is most commonly described in terms of a huge flux rope that is anchored to the Sun at both ends (Fig. 1). This concept is based on the observations of so-called magnetic clouds in the solar wind that exhibit smooth

* Corresponding author. Tel.: +358 408255529.
E-mail address: emilia.kilpua@helsinki.fi (E.K.J. Kilpua).

1364-6826/$ - see front matter © 2010 Elsevier Ltd. All rights reserved.
doi:10.1016/j.jastp.2010.10.012

rotation of the magnetic field through a large angle with enhanced magnetic field and depressed proton temperature (Burlaga et al., 1981). Goldstein (1983) first proposed that magnetic clouds could be locally modelled as cylindrically symmetric flux tubes with force-free magnetic fields, fulfilling $\nabla \times \mathbf{B} = \alpha \mathbf{J}$, where $\mathbf{B}$ is the magnetic field magnitude, and $\mathbf{J}$ the electric current density. It was noted few years later that a linear (i.e. constant α) solution describes rather well the magnetic field directional changes within magnetic clouds (Burlaga, 1988; Lepping et al., 1990, 2006). The solution in this geometry is based on the work by Lundquist (1950) and it describes magnetic field lines as a family of helices whose pitch angle increases with growing distance from the center of the flux rope. It is now widely appreciated that the Lundquist flux rope solution is only a first-order approximation and several extensions to the model have been developed over the years including non-constant alpha (Marubashi, 1986), the effect of expansion (Marubashi, 1997), uniform-twist (Farrugia et al., 1999), and non-force free effects (Mulligan and Russell, 2001; Cid et al., 2002; Hidalgo et al., 2002).

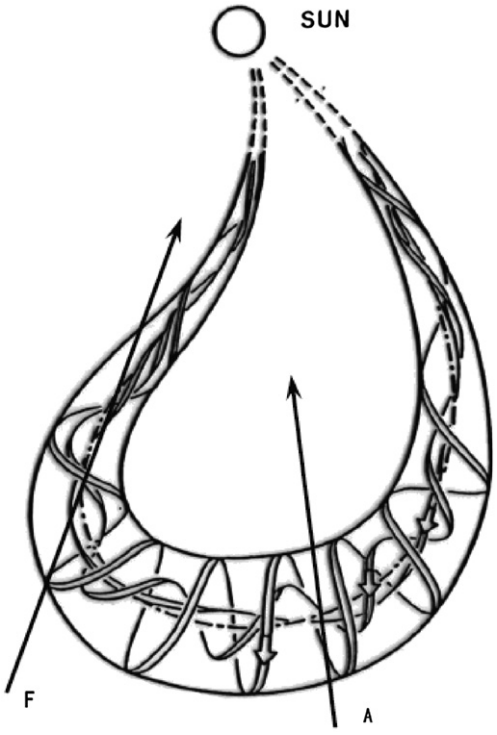

Fig. 1. Flux rope curved along the Parker spiral (Marubashi and Lepping, 2007).

Based on the behavior of the north–south component of the magnetic field, Mulligan et al. (1998) divided ICMEs to bipolar and unipolar ICMEs. In bipolar ICMEs the north–south component changes the sign within the ICME, while in unipolar ICMEs the north–south component maintains its sign. The division of ICMEs to unipolar and bipolar reflects the tilt of the flux rope axis with respect to the ecliptic plane. Bipolar ICMEs have low inclination while unipolar ICMEs are orientated roughly perpendicular to the ecliptic plane. By labeling the direction of the magnetic field at the boundaries and at the center of the ICME, Mulligan et al. (1998) presented eight flux rope categories (Fig. 2): SEN, SWN, NES, and NWS to present bipolar ICMEs, and WNE, ESW, ENW, and WSE to present unipolar ICMEs. For examples, in the SEN type ICME the field rotates from the south (S) at the leading edge to the east (E) at the center and finally to the north (N) at the trailing edge. Fig. 2 also shows the helicity of the magnetic field associated with each flux rope category. In the right-handed (RH) ICMEs the magnetic field

Magnetic Cloud Type	SEN	SWN	NES	NWS
Leading Field	South (-Bz)	South (-Bz)	North (+Bz)	North (+Bz)
Axial Field	East (+By)	West (-By)	East (+By)	West (-By)
Trailing Field	North (+Bz)	North (+Bz)	South (-Bz)	South (-Bz)
Helicity	LH	RH	RH	LH

Magnetic Cloud Type	WNE	ESW	ENW	WSE
Leading Field	West (-By)	East (+By)	East (+By)	West (-By)
Axial Field	North (+Bz)	South (-Bz)	North (+Bz)	South (-Bz)
Trailing Field	East (+By)	West (-By)	West (-By)	East (+By)
Helicity	RH	RH	LH	LH

Fig. 2. The flux rope categories for bipolar ICMEs (top) and for unipolar ICMEs (bottom). The figures are from the Mulligan et al. (1998) work.

rotates counterclockwise and in the left-handed (LH) ICMEs the rotation is clockwise.

In the interplanetary medium the appearance of ICMEs varies greatly and only about 1/3 of ICMEs close to the orbit of the Earth can be described as magnetic clouds (Gosling, 1990). However, as Jian et al. (2006) pointed out the absence of a flux rope in the majority of ICMEs does not imply that they do not have a central flux rope. Their analysis of total perpendicular pressure profiles (See Section 3.1) within ICMEs suggests that in about one-third of the cases the spacecraft traverses the ICME's central flux rope but in the majority of the cases the spacecraft encounters the ICME disturbance sufficiently far from the center that the central rope is not identifiable.

The characteristics and the number of identified ICMEs correlate with the phase of the solar cycle. The monthly ICME rate (determined from single spacecraft observations near 1 AU close to the ecliptic plane) increases by about one order of magnitude from one event every three months at solar minimum to one event per week at solar maximum (Richardson and Cane, 2004a; Jian et al., 2006; Riley et al., 2006). Interestingly, the fraction of magnetic clouds among all ICMEs depends on the solar activity levels (Richardson and Cane, 2004b; Huttunen et al., 2005; Riley et al., 2006) being about one order of magnitude larger at solar minimum than at solar maximum. This is consistent with the work by Jian et al. (2008a, 2010) who found that at solar minimum, the ICMEs are generally smaller and weaker than other solar cycle phases, and a higher fraction of ICMEs are encountered by the spacecraft through the central flux rope than simply through a disturbed region surrounding it.

The occurrence rate of the observed flux ropes could be modified by the migration of CME source regions towards the poles near solar maximum (Huttunen et al., 2005; Jian et al., 2008a; Riley et al., 2006). As a consequence more ICMEs are traversed far from the center by the spacecraft that are located close to the ecliptic plane. In addition, at solar maximum the interaction between multiple CMEs may lead to a "complex ejecta" where individual characteristics of ICMEs are no longer visible (Burlaga et al., 2002). It is also possible that active region CMEs, which are more common at solar maximum, have more complicated structure than CMEs associated with the quiescent filaments and streamer blowouts (e.g., Maia et al., 2003). At solar maximum ICMEs on average have larger radial diameters and higher magnetic fields than near solar minimum (Richardson and Cane, 2004a; Jian et al., 2006). In addition, ICMEs are somewhat faster and they drive interplanetary shocks more often at 1 AU during the years of high solar activity.

It is also well-established that the flux rope structure (Fig. 2) of magnetic clouds varies systematically with the solar cycle (e.g., Mulligan et al., 1998; Bothmer and Schwenn, 1998; Huttunen et al., 2005; Li and Luhmann, 2004). During the odd numbered solar cycles magnetic field within bipolar ICMEs rotates predominantly from the south to the north while during the even cycles the rotation is reversed. The dominant polarity changes in the late declining phase of the solar cycle (Li and Luhmann, 2004). Mulligan et al. (1998) also indicated that the ICME orientation depends on the solar activity cycle. In the declining phase most ICMEs were unipolar while during the year of high solar activity most ICMEs were bipolar. They suggested that while the leading magnetic field polarity is controlled by the polarity of the Sun's global field the ICME orientation is controlled by the inclination of the coronal streamer belt.

The basic flux rope model assumes that ICMEs are in equilibrium and have circular cross-sections. However, as shown by several studies, ICMEs are dynamic structures that undergo extensive expansion and interact strongly with the ambient solar wind that will lead to the distortion of the magnetic field pattern and oblate cross-sectional shapes (e.g., Gosling, 1990; Farrugia et al., 1995; Mulligan et al., 1999; Mulligan and Russell, 2001; Russell and Mulligan, 2002; Riley and Crooker, 2004; Lepping et al., 2006; Liu et al., 2006). The expansion shifts the magnetic field maximum from the center towards the leading edge and results in declining speed profiles and the increase in the ICME size with solar distance (Gosling, 1990). On the other hand, the compression by the overtaking high speed stream leads to the magnetic field and speed profiles that peak towards the trailing portion of the ICME. Russell and Mulligan (2002) present observational evidence against the cylindrically symmetric flux rope model. Their analysis showed that the shock stand-off distances ahead of ICMEs are much greater than what would be produced by the spherical object and they discussed the distribution of the impact parameters (closest approach from the flux rope axis) and shock normal orientations as well as the multi-spacecraft observations. As it will be discussed in more detail in Section 2 multipoint observations have indicated several cases where the spacecraft encountering the same ICME have been separated by distances that were larger than the radial width of the ICME.

Vandas et al. (1993a) presented magnetic force-free solutions using a spheroidal geometry for oblate, prolate and spherical magnetic clouds and examined their magnetic field configurations. In a spheroidal model a magnetic cloud is considered as a closed bubble completely detached from the Sun. Spheroidal magnetic cloud topologies offer more flexibility to fit complex magnetic field profiles than the cylindrically symmetric flux rope solution (Vandas et al., 1993a,b). These studies also showed that spheroidal topologies can explain the occasional double flux ropes in the solar wind with full sinusoidal profiles of magnetic field components and double-peak magnetic field magnitude profiles. However, as indicated by the studies of the polytropic index in expanding magnetic clouds, the spheromak configuration seems an implausible model for magnetic clouds (Farrugia et al., 1995). In addition, when the effect of expansion is added to the cylindrical flux rope model it can explain many asymmetries in the observed magnetic field profiles (Farrugia et al., 1995; Vandas et al., 2005; Owens et al., 2006). Double flux rope configurations can also be explained in terms of two separate flux ropes erupting from the same source region on the Sun within a short time interval or by the spacecraft traversing twice through the axis of a deformed single flux rope bent back onto itself in a Parker spiral like fashion (Rees and Forsyth, 2004; Marubashi and Lepping, 2007).

The bent flux rope shown in Fig. 1 presents a closed magnetic field topology with the field lines attached to the Sun at both ends. It has also been proposed that ICMEs would be completely detached from the Sun in the form of a bubble like plasmoid or even a torus (e.g., Ivanov et al., 1989; Gosling, 1990; Vandas et al., 1993a). Closed magnetic field structures are characterized in the solar wind by oppositely flowing suprathermal electron beams (Gosling et al., 1987; Gosling, 1990). However, the detection of energetic flare associated electrons within magnetic clouds support the magnetic connection to the Sun beyond 1 AU (Farrugia et al., 1993; Malandraki et al., 2000) as suggested by the flux rope topology where field lines are still rooted at the Sun. Even though a torus is not a likely model to present the large-scale configuration of magnetic clouds, the toroidal model has been successfully used to take into account the curvature effect in a case where the spacecraft traverses close to the leg of the bent flux rope loop (Marubashi and Lepping, 2007).

A different approach to interpret magnetic clouds has been developed by Hu and Sonnerup (2002). They use magnetic field and plasma measurements collected along the spacecraft trajectory through a magnetic cloud to solve the non-linear Grad–Shafranov (GS) equation in a plane perpendicular to an invariant direction. The advantages of the GS technique are that it does not assume a force-free configuration and does not constrain the cross-section shape. The method recovers the 2.5 dimensional cross-section in a

plane perpendicular to the invariant axis. However, this technique assumes that the analyzed structure is in magnetostatic equilibrium that may lead to the underestimation of the distortion of the magnetic cloud's shape (Riley et al., 2004).

Due to the huge dimensions of ICMEs, multi-spacecraft observations with the spacecraft separated at least by few degrees are necessary to study the large-scale ICME properties. The majority of ICME observations come from single-spacecraft encounters and as a consequence the knowledge of the three-dimensional structure of ICMEs is still rather poorly understood. One of the main scientific goals of the Solar TErrestrial RElation Observatory (STEREO) (Kaiser et al., 2007), launched in late 2006, is to increase our understanding of the global structure of ICMEs. STEREO consists of two functionally identical satellites, one that leads the Earth (STEREO A; STA), and one that lags the Earth (STEREO B; STB) in its orbit around the Sun with gradually increasing angular separation. The STEREO spacecraft carry instruments (SECCHI and SWAWES packages) to remotely sense CMEs and their shocks by white-light and radio waves as well as instruments (IMPACT and PLASTIC packages) to identify and study ICMEs in situ in the interplanetary medium. STEREO observations can be combined with the corresponding observations from the Lagrangian point L1 (ACE, WIND and SOHO), approximately between the STEREO spacecraft. Before the STEREO mission there have been occasional fortunate constellations of spacecraft allowing probing the large-scale structure of ICMEs (see Section 2.1).

In this review we will summarize the multi-spacecraft ICME studies conducted before the STEREO mission (Section 2) and discuss the multipoint ICME observations during a one-year period from April 2007 through March 2008 using observations from the STEREO and L1 spacecraft (Section 3). In particular, we will discuss the constraints on the global scale-sizes of ICMEs deduced from these observational studies. In Sections 4 and 5 we will discuss and summarize our results.

2. Pre-STEREO multi-spacecraft ICME observations

Although STEREO is the first mission that was particularly designed to make multi-spacecraft ICME observations there have been several reported cases before the launch of the STEREO spacecraft when two or more spacecraft encountered the same ICME. In this review particular attention is paid to ICMEs that were observed by spacecraft separated in longitude near the ecliptic plane, although configurations where the spacecraft are separated radially or in latitude also provide important information about the evolution and global morphology of ICMEs. As illustrated in Fig. 3 depending on the tilt of the flux rope axis with respect to the ecliptic plane, the longitudinal separation between the spacecraft serves as the measure either for the transverse extent of the flux rope loop (low inclination ICME) or for the cross-section thickness (high inclination ICME).

Radial evolution of ICMEs as they propagate from the Sun to the outer heliosphere has been studied using observations from Ulysses, Pioneer Venus Orbiter (PVO), Helios and Voyager spacecraft combined with the observations near the orbit of the Earth (e.g., von Steiger and Richardson, 2006; Liu et al., 2005; Richardson et al., 2006; Foullon et al., 2007; Jian et al., 2008b, and references therein). The changes in the ICME structure with heliospheric distance are, in particular, important for estimating the influence of ICMEs on the environment of other planets and studying their consequences to the large-scale solar wind structure in the heliosphere. The work by Jian et al. (2008b) investigated the radial evolution of ICMEs by comparing the properties of ICME at 5.3 AU by Ulysses with the ICME observations at 0.72 AU by PVO (Jian et al., 2008a) and at 1 AU by Wind and ACE (Jian et al., 2006), while Jian et al. (2008c) studied the variations of ICME properties within the short distances from 0.72 to 1 AU. They considered carefully the effect of the solar cycle variations and in addition, all observations were conducted close to the ecliptic plane to minimize the latitudinal variations. The study indicated that while the ICME width increases with the heliospheric distance from the Sun, the expansion weakens significantly from 1 to 5.3 AU. Only the strongest CMEs can expand in radial width up to distances of several tens of astronomical units (Richardson et al., 2006; von Steiger and Richardson, 2006). Furthermore, Jian et al. (2008b) showed that the decrease in the magnetic field magnitude and in total perpendicular pressure with the distance from the Sun is stronger in ICMEs than in the ambient solar wind or in the stream interaction regions. As a consequence, the identification of ICMEs gets more difficult at larger heliospheric distances. However, a few ICMEs have been tracked with the aid of the alpha enhancement and one-dimensional MHD simulation to Voyager 2 up to heliospheric distance of 70 AU (Paularena et al., 2001; Richardson et al., 2006; von Steiger and Richardson, 2006).

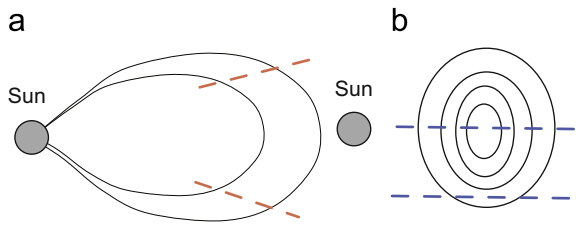

Fig. 3. Estimating the ICME scale-size in a case of (a) a low inclination flux rope and (b) a flux rope with axis perpendicular to the ecliptic plane. The sketches present the projection of the flux rope loop (a) and the cross-section (b) in the ecliptic plane. The dashed lines indicate the possible spacecraft trajectories.

The latitudinal extent and the off-ecliptic structure of ICMEs have been studied by combining observations from Ulysses with the measurements near the ecliptic plane (see von Steiger and Richardson, 2006, and references therein). Reisenfeld et al. (2003) reported ICMEs that extended from the northern coronal hole at about 70° in latitude all the way to the ecliptic plane. The studies made at large latitudinal separations have indicated differences in the shock formation, driving force of the ICME and the ICME structure (Gosling et al., 1995, 1998; Reisenfeld et al., 2003; Riley et al., 2003) when compared to the ICMEs observed closer to the ecliptic plane. For example, observations by Gosling et al. (1995, 1998) showed that an ICME can drive a strong forward shock at the ecliptic, but at high latitudes a weak forward–reverse shock pair was detected. The authors concluded that in the ecliptic plane the main driver of the ICME is the speed difference between the CME and the slower ambient solar wind while at higher latitudes the CME expansion plays a significant role. An alternative explanation for the forward–reverse shock pairs associated with high latitude CMEs was provided by Manchester and Zurbuchen (2007) who proposed that the reverse shock would form as a result of deflection of the solar wind caused by the passage of the CME. Using ICMEs identified by both ACE and Ulysses when the spacecraft were separated from 40° to 70° in latitude, Liu et al. (2006) estimated the cross-section aspect ratio to be no smaller than 1:6. This is consistent with the corresponding aspect ratios obtained from kinematic studies and simulation works (e.g., Riley and Crooker, 2004; Manchester et al., 2004).

The curved flux rope model was originally based on the multi-spacecraft study by Burlaga et al. (1981, 1990) who combined observations from four spacecraft (IMP-8, Helios A and B, Voyager 2) located close to the ecliptic plane at heliospheric distances ranging between 1 and 2 AU and separated up to several tens of degrees in longitude. The flux rope axis was estimated to be lowly inclined at all locations using the cylindrically symmetric model. IMP-8 and Helios A traversed the loop from the opposite boundaries (see Fig. 3 in Burlaga et al., 1990) and thus the angular separation between IMP-8 and Helios A, about 30°, gives the lower limit estimate for the longitudinal span of the flux rope.

Crooker and Intriligator (1996) studied a magnetic cloud on October 1974 observed by IMP 6–8 near the Earth and by Pioneer 11 located 30° in longitude and 4.8 AU in the radial direction away from the IMP spacecraft. Despite the large angular separation between the spacecraft very similar magnetic field signatures, nearly identical radial widths and similar sector boundary crossings were observed at both locations. The investigated magnetic cloud had high inclination (about 60°) and thus the longitudinal separation between the spacecraft provides an approximation for the length of the magnetic cloud cross-section. It was concluded that the length of the cross-section exceeded the radial width by at least a factor of 8, i.e. the aspect ratio (the ratio of the radial width to the longitudinal thickness) was at least 1:8. The studied magnetic cloud was compressed by a second ICME that likely contributed to the highly elongated cross-section shape and exhibited its radial expansion.

The Earth flyby of the Near Earth Asteroid Rendezvous (NEAR) spacecraft in early 1998 combined with the Wind observations allowed Mulligan et al. (1999) to conduct a multi-spacecraft study of four ICMEs with the angular separations from 1.2° to 33.4° in longitude. When the spacecraft were very close to each other ($\sim 1°$) they detected very similar magnetic field signatures, but distinct differences were already apparent when the spacecraft separation had increased to 5.4°. However, the helicity of the identified magnetic cloud was same for all cases at the two locations. As noted by Mulligan et al. (1999) this supports the idea of the bent flux rope topology in which the direction of the axial field depends upon the location at which it is sampled, but in which the helicity remains the same. We will discuss the scale-sizes of these magnetic clouds in Section 2.1.

Mulligan and Russell (2001) used Pioneer Venus Orbiter (PVO) and ISEE 3 observations to investigate the structure of an ICME observed on August 27, 1978. The spacecraft were separated by only 0.02 AU radially and by 12° (0.21 AU) in longitude. The authors applied the force-free cylindrically symmetric model and the non-force free longitudinally stretched model. Both models fit successfully to the data, but the cylindrically symmetric model returned flux rope diameters that were smaller than the longitudinal separation between the spacecraft. The other model returned a single stretched flux rope with high inclination (74°) and the cross-section aspect ratio about 1:4. The non-cylindrical model did not assume force-free field, but only slight deviations were observed from the force-free configuration.

2.1. The scale-sizes of ICMEs in the Mulligan et al. (1999) work

We estimate next the scale-sizes for the magnetic clouds studied by Mulligan et al. (1999). These events were identified by Wind and NEAR with angular separations 1.2° (Event M1: December 10–11, 1998), 5.4° (Event M2: November 22–23, 1998), 11.3° (Event M3: November 7–8, 1998), and 33.4° (Event M4: September 21–24, 1998) in longitude. We discuss only Events 2–4 since during Event 1 the spacecraft separation was so small that no significant differences in the ICME structure were detected. The flux rope axis orientations are not given in the paper, but we refer to the inclination angles at Wind indicated in the magnetic cloud list in Huttunen et al. (2005). The conclusions about the magnetic structure and the spacecraft crossing distances from the apex of the flux rope loop are from the Mulligan et al. (1999) work. Note that the radial separation of Wind and NEAR that varied from 0.18 AU (Event M1) to 0.63 AU (Event M4) might have contributed to the observed differences in the ICME structure between the spacecraft.

Event M2: This was a clear ICME at Wind embedded in a leading edge of a high speed stream. The radial diameter of the ICME (d_{CL}), obtained by multiplying the ICME duration by the average speed in the ICME, was 0.20 AU. It was concluded that NEAR encountered the same ICME, but there were strong dissimilarities in the magnetic field components between the spacecraft although the spacecraft separation was only 5.4° (0.094 AU). For example, Fig. 3 in Mulligan et al. (1999) shows that the north–south magnetic field component maintained negative polarity throughout the ICME at Wind, but in the NEAR data it was positive. At Wind the ICME had a clear flux rope structure with its axis perpendicular to the ecliptic plane, but at the location of NEAR the ICME was less rope-like and it was difficult to assign its helicity. The magnetosheath region preceding the ICME at Wind was shorter than at NEAR suggesting that Wind traversed closer to the nose of the ICME than NEAR. The magnetic field magnitude was also higher at Wind than at NEAR. If we assume that Wind traversed through the center of the flux rope and NEAR close to its boundary, the ICME extent in the east–west direction was about 0.20 AU suggesting almost a circular cross-section. However, this gives only a minimum bound for the cross-section and the true cross-sectional shape is likely more elongated. Mulligan et al. (1999) propose that lower magnetic field and thicker sheath region at NEAR than what were observed at Wind could also result from the expansion of the ICME from ~ 1 to 1.3 AU. In addition, although it seems clear that the spacecraft went through the same ICME, significant differences in the magnetic field components suggest that the spacecraft perhaps encountered different structures within the ICME or that the ICME was highly distorted. As a result, this further complicates the conclusions one can make about the cross-sectional shape.

Event M3: A clear flux rope ICME was observed both at Wind and at NEAR. The ICME had low inclination at the location of Wind and the radial width of 0.18 AU. From the observations it was difficult to determine which spacecraft traversed closer to the apex of the ICME. Both spacecraft observed clear magnetic field rotation, but the magnetic field rotation pattern was quite dissimilar. As suggested by Mulligan et al. (1999) the spacecraft likely traversed through different structures within the ICME. This ICME extended at least 11.3° in longitude, but presumably the flux rope was considerably wider since magnetic cloud signatures were clear at both spacecraft.

Event M4: Wind identified a clear ICME with coherent magnetic field rotation. This high inclination ICME was embedded within a slow speed solar wind and had the radial width of 0.18 AU. The ICME at NEAR had a much lower magnetic field magnitude than what was observed at Wind. NEAR detected clear magnetic field rotation, but there were significant dissimilarities in the magnetic field components between the spacecraft. Fig. 5 in Mulligan et al. (1999) indicates that within the ICME the north–south magnetic field components had opposite polarities between the spacecraft and the east–west component rotated from positive to negative at Wind, but from negative to positive at NEAR. The helicity of the ICME was left-handed at both spacecraft. Wind and NEAR were separated by 0.58 AU in the east–west direction. Since the observations suggest that Wind traversed the ICME substantially closer to the apex than NEAR, the separation between the spacecraft gives an estimate for the half thickness of the flux rope cross-section. This would imply a significantly elongated cross-section, with the aspect ratio of 1:6.4. We again emphasize that these conclusions depend on the large-scale geometry of the ICME. Mulligan et al. (1999) further point out that when the spacecraft separation is large, one cannot be confident that the spacecraft went through the same ICME. In any case, if Wind and NEAR encountered the same overall structure, the observations suggest that the ICME was highly distorted.

3. Multi-spacecraft study: STEREO and L1 observations

3.1. Methods and used data

The advantage of STEREO observations compared to the previous multi-spacecraft ICME studies described in Section 2 lies in

the quality of measurements and in the gradual increase of the spacecraft separation angle ($\sim 45^{\circ}$ per year). STEREO was launched at the brink of the long and deep solar minimum. Despite the low solar activity several ICMEs have been identified in the solar wind (see Kilpua et al., 2009a and the UCLA ICME list at http://www-ssc.igpp.ucla.edu/forms/stereo/stereo_level_3.html), but the majority of them have had relatively low magnetic field magnitudes and/or small radial diameters.

In this section we will investigate multi-spacecraft ICME encounters using observations from the STEREO spacecraft and the L1 spacecraft (Wind and ACE) during the one-year interval from April 2007 through March 2008. During this time interval the separation between the STEREO and L1 spacecraft was large enough to study the global ICME structure and small enough that multi-spacecraft encounters were likely. In the beginning of April 2007 STEREO spacecraft were separated by 3° and by the end of March 2008 the separation had increased to 48°. The ICME intervals and some of their characteristic parameters are given in Table 1.

We use the ICME list published in Kilpua et al. (2009a) as a starting point. This list includes ICMEs that had clear magnetic field signatures (organized magnetic field behavior and depressed levels of magnetic field fluctuations), maximum magnetic field magnitude above 5 nT and duration at least 3 h. Between April 2007 and March 2008 the list includes 10 events from which four are listed as multi-spacecraft encounters. In this paper we conduct a more detailed analysis of these multi-spacecraft events and perform a careful search for the ICME signatures at the other two locations for the single-spacecraft encounters. The purpose is to identify events, where one spacecraft detected a clear ICME and the other spacecraft crossed just the flanks of the same ICME. We search for any ICME signatures (listed in the next paragraph) and do not set any constraints for the magnetic field or the duration of the ICME. The magnetic field measurements are given in the RTN coordinate system where R denotes the direction away from the Sun to the spacecraft, T is parallel to the rotational equatorial plane of the Sun, directed in the sense of rotation and N completes the right-handed triad ($\mathbf{N} = \mathbf{R} \times \mathbf{T}$).

Identification of ICMEs is sometimes problematic (e.g. Gosling, 1997; Zurbuchen and Richardson, 2006) as there is no signature present in all ICMEs and different signatures do not always occur simultaneously and may be present intermittently during a given ICME. We consider here the following signatures: enhanced magnetic field magnitude, smooth variation of the magnetic field direction, depressed level of magnetic field fluctuations, depressed proton temperature and proton beta, and the intervals of bidirectional suprathermal electrons (BDE). We study the magnetic field structure of ICMEs by visual inspection of the data. We divide ICMEs into bipolar and unipolar flux rope categories indicated in Fig. 2. It should be noted that due to irregular magnetic field changes we cannot assign the flux rope category and helicity for all investigated ICMEs.

In addition, we investigate the profiles of the total pressure (sum of the magnetic pressure and plasma thermal pressure) perpendicular to the magnetic field. Russell et al. (2005) first presented this simple parameter as a useful tool to help identify ICMEs from the ambient solar wind measurements and to estimate the closest approach of the spacecraft from the core of the ICME. A study of 230 ICMEs during 1995–2004 by Jian et al. (2006) divided ICMEs into three categories according to their total perpendicular pressure (P_t) profiles. In *Group*1 the P_t profiles display clear central enhancement and represent ICMEs that are traversed near the center. *Group*3 includes ICMEs crossed far from the center and they show a rapid increase followed by gradual decay in P_t. The P_t profiles of *Group*2 ICMEs show steady plateau and in this group ICMEs are crossed at intermediate distances from the center. We have indicated the group to which each ICME belongs in Table 1.

The location of the ICMEs with respect to the large-scale solar wind sector structure is also an important aspect when comparing the observations between the widely separated spacecraft. The magnetic field sector boundary crossings (SBC) are determined by the change of the magnetic field azimuthal (ϕ_B) component from the away to the towards sector or vice versa. The away sector refers to magnetic field lines that point away from the Sun, in the RTN coordinate system corresponding the azimuth direction within $225-45^{\circ}$ ($\phi = 0^{\circ}$ points away from the Sun and $\phi = 90^{\circ}$ is defined westward in RTN). In the towards sector magnetic field lines point to the Sun and the azimuth angle is within $45-225^{\circ}$. In the away sector the solar wind heat flux flows along the magnetic field lines (pitch angles near 0°), while in the towards sector the heat flux flow is anti-parallel to the magnetic field (pitch angles near 180°).

3.2. Identified multi-spacecraft ICME encounters

We discuss in the following only ICMEs for which we were able to find clear indications of the possible multi-spacecraft encounters. This was the case for six events of the 10 investigated ICMEs. For the remaining events we could not find any ICME related signatures at the other spacecraft or the signatures were very unclear.

3.2.1. Events 1–2: May 21–23, 2007

The first multi-spacecraft ICME encounters during the investigated interval occurred on 21–22 May, 2007 (Event 1) and on 23 May, 2007 (Event 2). The general properties of these magnetic clouds as well as the surrounding solar wind structure and their CME sources are described in detail in Kilpua et al. (2009b). The STEREO separation at that time was about 9°. The first magnetic cloud was crossed through the center by STB while Wind encountered the cloud about $0.3d_{CL}$ (where d_{CL} is the cloud's diameter) from the axis. Presumably, STA made a glancing encounter through the ICME. The separation between Wind and STB was only three

Table 1
Multipoint ICME encounters from April 2007 through March 2008. The columns give: event number (N), time when the front boundary of the ICME arrived at each spacecraft (A: STA, W:Wind, B: STB), longitudinal separation between the STEREO spacecraft, duration of the ICME (dt), maximum magnetic field (B_{max}), average solar wind speed within the ICME (V_{ave}), helicity (LH stands for left-handed and RH for right-handed magnetic field rotation). The next column indicates the group the ICME belongs according to its total perpendicular pressure profile (see Section 3.1). "nc" indicates not clear.

N	T_{IA}	T_{IW}	T_{IB}	ϕ_{AB}	dt (h)	B_{max} (nT)	V_{ave} (km/s)	Helicity	Group
	2007								
1	5/21 1910	5/21 2245	5/22 0425	9.0	6.2,17.1,17.7	9.9,14.8,17.6	482,456,447	RH,RH,RH	nc,1,1
2	5/23 0056	5/23 0950	–	9.0	11.5,3.7,–	11.8,10.1,–	497,500,–	RH,RH,–	2,nc,–
3	11/19 2224	11/19 2310	11/19 2255	40.8	25.2,11.9,7.7	12.3,19.4,17.2	417,477,455	LH,LH,LH	2,1,nc
4	12/25 2230	12/25 1550	–	43.6	7.9,18.6,–	5.3,6.2,–	428,360,–	nc,LH,–	2,1,–
5	–	12/30 2150	12/30 0615	43.9	–,10.4,44.3	7.4,13.8,–	–,320,314	–,nc,RH	–,nc,1
	2008								
6	3/8 1820	3/8 1745	–	46.3	12.3,7.0,–	11.8,14.0,–	399,390,–	LH,LH,–	2,nc,–

degrees and although the general behavior of the magnetic field components was similar, clear differences were apparent. The flux rope signature (smooth magnetic field rotation, depressed temperature) was evident at STB and Wind, while at STA the ICME structure was clearly more complex. The ICME leading edge arrived first to STA, then at Wind and finally at STB. The 23 May magnetic cloud was encountered $\sim 0.3 d_{CL}$ west of the axis by STA and close to its eastern edge by Wind, located almost 6° from STA. STB did not observe this event. Observations indicate clear flux rope at STA, but at Wind the magnetic field changes were much less organized.

The Grad–Shafranov (GS) reconstruction indicated that both May 2007 magnetic clouds were right-handed and had high inclination (Liu et al., 2008; Kilpua et al., 2009b; Möstl et al., 2009a,b). Furthermore, the GS technique yielded rather circular cross-sections with the aspect ratios roughly 1:1.5 (Möstl et al., 2009a,b), It should be noted that for the 21–22 May magnetic cloud the GS map did not extend to the location of STA. If it is assumed that STA encountered the flanks of the magnetic cloud, as suggested by the observations, the aspect ratio is somewhat larger, about 1:2. As indicated by the GS reconstruction the flux rope geometry was well validated for these magnetic clouds (Liu et al., 2008; Möstl et al., 2009a,b). For the May 23 magnetic cloud, Möstl et al. (2009b) found that the magnetic cloud was non-force free in about a quarter of the cloud and that the cloud had almost a constant twist, i.e. not consistent with the Lundquist solution where the twist of the field lines decreases from boundaries to the core.

Both magnetic clouds were bounded by high speed solar wind streams. There were no SBCs in the immediate vicinity of the 21–22 May magnetic cloud, but the magnetic field changed from the away to the toward sector at the end boundary of the 23 May magnetic cloud at STA and at Wind. The time of the heat flux reversal is difficult to determine due to the BDE signature associated with the following high speed stream. BDEs are commonly observed in the vicinity of high speed streams. Electrons are energized at the shocks/pressure waves that bound the compression region that is formed when the high speed stream overtakes the slower solar wind. The energized electrons leak out from the compression region and produce field-aligned electron beams directed away from the compression region on both sides (Steinberg et al., 2005).

3.2.2. Event 3: November 19–20, 2007

The next clear multi-spacecraft ICME encounter occurred on November 19–20, 2007. This event is described in Howard and Tappin (2009) in a third part of the paper series aiming to connect the in situ ICME structure to the simulated image of ICMEs based on the observations by the heliospheric imagers onboard the STEREO spacecraft (HI) and the Coriolis (SMEI) spacecraft. The ICME was merged at the leading edge of a corotating interaction region (CIR) and this combined structure was observed at all considered locations (STA, STB and L1). The ICME was fast enough to drive an interplanetary shock that was detected at STB 3.5 h before it arrived at L1, although the L1 spacecraft are located 0.04 AU closer to the Sun than STB. At STA no clear shock was identified.

Fig. 4 shows observations from L1 (ACE and Wind), STB and STA. At L1 coherent magnetic field rotation and a smooth magnetic field profile were observed. The compression by the following high speed stream is featured by the magnetic field magnitude and speed profile that peak towards the trailing edge. STB recorded more complex magnetic field structure than what was observed at L1. The middle panels of Fig. 4 show a double peaked magnetic field profile and similar double drop structures in the temperature and plasma beta. Although Howard and Tappin (2009) concluded that the ICME was not observed at STA we identified from the STA measurements a region during which the magnetic field rotation resembles closely the magnetic field changes at L1. The rotation in the radial component is opposite between the spacecraft, but the

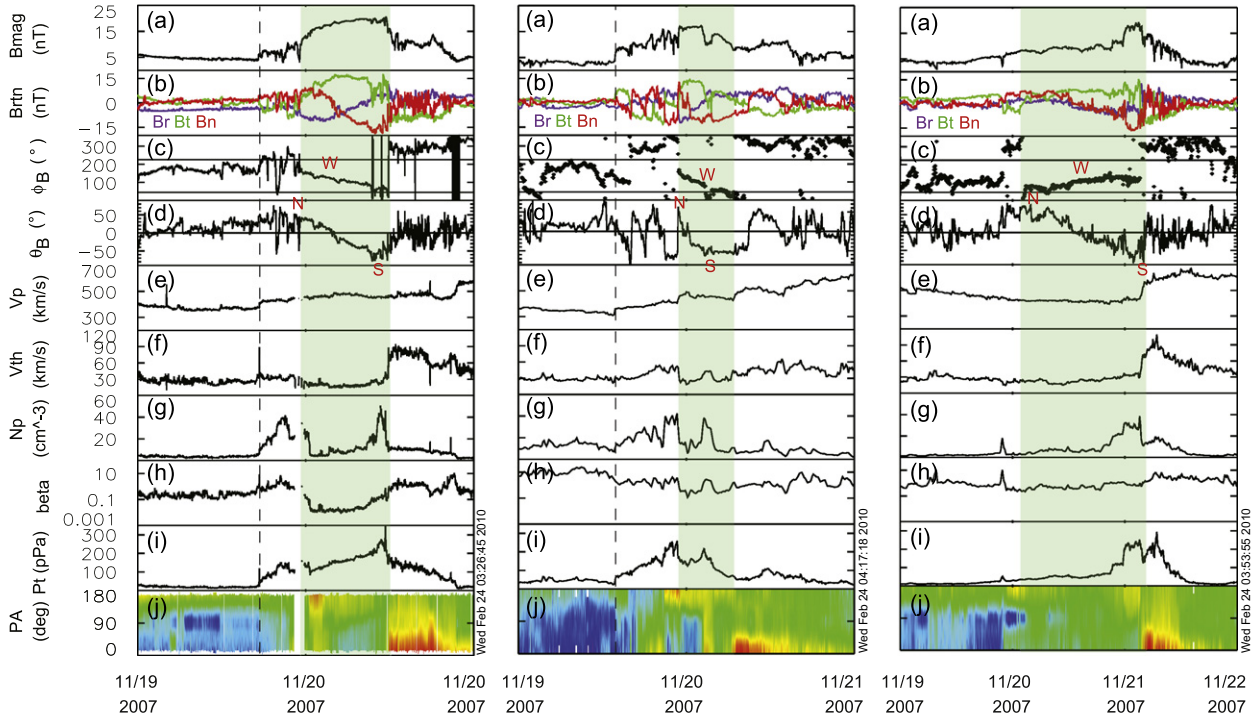

Fig. 4. Left: ICME observed at L1 between 19 November 2007 2310 UT–20 November 2007 1145 UT. Middle: ICME observed at STB between 19 November 2007 2255 UT–20 November 2007 0645 UT. Right: ICME observed at STA between 19 November 2007 2224 UT–21 November 2007 0435 UT. The panels show from top to bottom: (a) magnetic field magnitude, (b) magnetic field components in RTN, (c) magnetic field longitude angle, (d) magnetic field latitude angle, (e) solar wind speed, (f) thermal speed, (g) density, (h) plasma beta, (i) total perpendicular pressure, and (j) suprathermal electron pitch angle spectrogram of 246 eV electrons (STEREO) and 260 eV (Wind). The green areas mark the ICME intervals and the dashed line indicates the interplanetary shock. At L1 the magnetic field observations are from ACE and the plasma and suprathermal electron data from Wind. (For interpretation of the references to color in this figure legend, the reader is referred to the web version of this article.)

changes in the other two magnetic field components follow the directional changes at L1.

We see from Fig. 4 that the magnetic field N-component rotates from the north to the south at all considered spacecraft. This signifies that the ICME was a bipolar magnetic cloud, i.e. its axis lay close to the ecliptic plane. The magnetic field longitude angle points roughly to the west ($\phi = 90^{\circ}$ in the RTN coordinates) at the center of the ICME. Thus, we identify this ICME as having a flux rope type NWS and left-handed helicity. Note that at STB the magnetic field rotation during the first magnetic field enhancement region, in particular, is similar the magnetic field changes at L1.

The spacecraft at L1 presumably traversed the ICME close to the center as suggested by the P_t profile. The P_t profile increases towards the trailing edge of the ICME due to the compression by the overtaking CIR but otherwise it resembles the Group 1 event (see Section 3.1). At STB the P_t profile is quite irregular and it is not possible to assign the P_t category. At STA the P_t profile shows a plateau (Group 2) with an increase in the end part due to the interaction with the overcoming fast solar wind.

Pitch angle spectrograms show that at STB and at L1 the heat flux flow was unidirectional within the ICME, while at STA bidirectional electron flow was identified. At STB an interval of weak bidirectional electron flow started at the trailing edge of the ICME and continued for 12 h. At all spacecraft there was a SBC from toward to away sector at the ICME trailing edge.

As discussed by Howard and Tappin (2009) the CME that produced this ICME erupted on 15 November 2007. The event appeared as a partial halo CME in the coronagraph observations at all three locations (STA, STB and at L1 in the LASCO instrument of the SOHO spacecraft), but it was most easily observed by STB. There were also two other significant CMEs observed close to this event on 14 November and 16 November. Both CMEs were clearly visible in the STB coronagraph images and the bulk CME material was concentrated on the west limb of the Sun.

Observations suggest that the same ICME was observed at all considered locations. However, one cannot rule out the possibility that the ICME at STA was produced by a different CME although the magnetic field directional changes were rather similar between the spacecraft. As concluded above, the L1 spacecraft encountered the magnetic cloud closest to the center. In addition, the magnetosheath region was thicker at STB than at L1, having durations of 9.2 and 6.5 h, respectively. If we assume that STA traversed the same ICME as the one detected at L1 and STB the separation between the STEREO spacecraft, 40.8° (0.86 AU), gives a lower limit estimate for the angular extent of this low inclination magnetic cloud. The ICME duration at STA was more than twice as long as at L1 and STB suggesting that STA might have traversed close to the leg of the flux rope.

3.2.3. Event 4: December 25–26, 2007

Fig. 5 shows measurements from the L1 spacecraft and STA on 25–26 December 2007 when the separation between the Earth and STA was 21.1° (0.37 AU). For this time period the Kilpua et al.

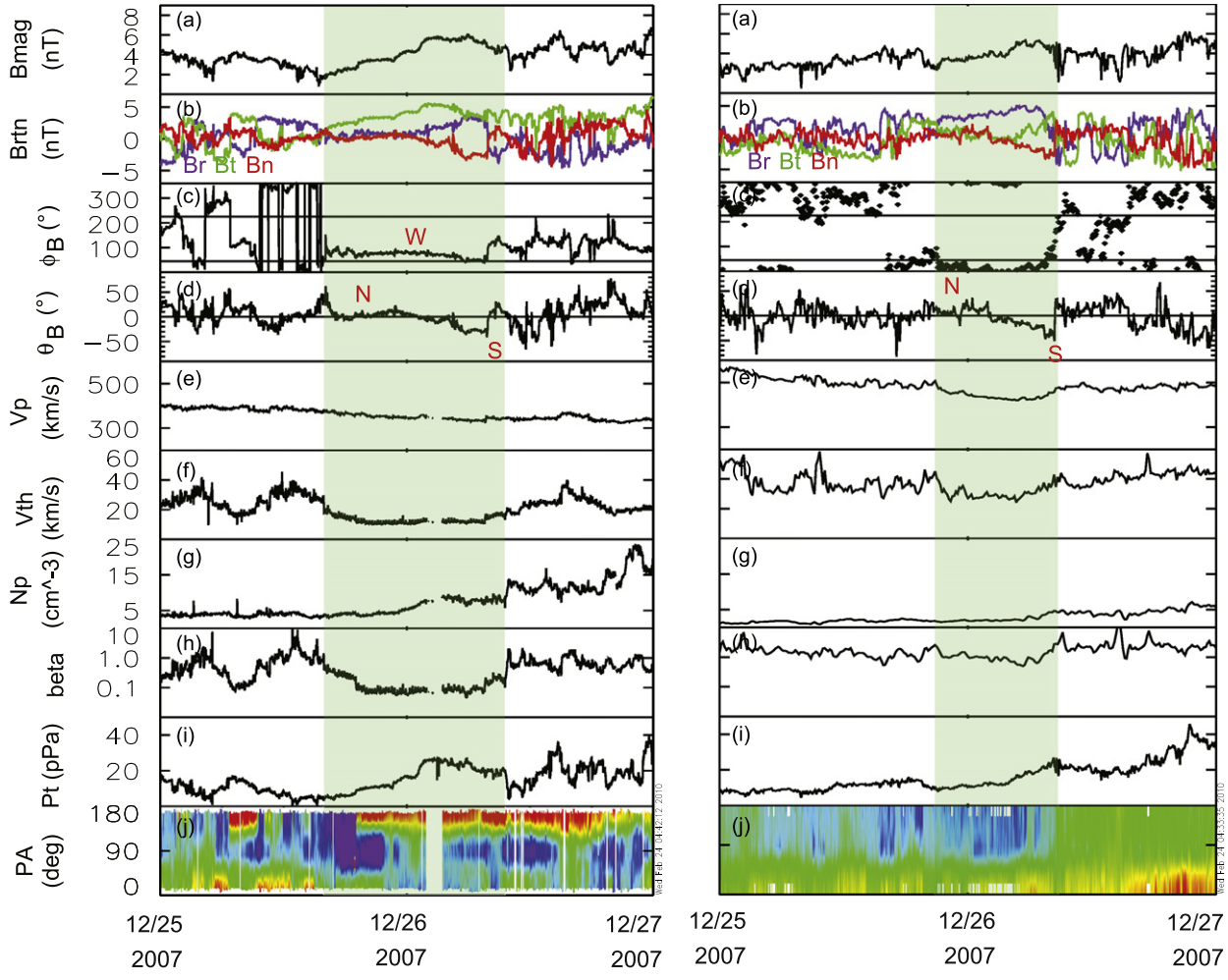

Fig. 5. Left: ICME observed at Wind between 25 December 2007 1550 UT–26 December 2008 0945 UT. Right: ICME observed at STA between 25 December 2230 UT–26 December 0850 UT. The panels are same as in Fig. 4.

(2009a) list has an ICME only at L1 where organized magnetic field behavior, depressed levels of magnetic field fluctuations and drops in the temperature and plasma beta mark the passage of the ICME past the spacecraft. We searched ICME signatures from the STA and STB measurements. At STB no ICME signatures were observed, but from the STA data we identified an interval during which the magnetic field directional changes roughly corresponded to those observed at L1. In addition, there were slight depressions in the temperature and plasma beta. The ICME duration at L1 was more than twice the duration at STA. The leading edge of the ICME arrived at L1 6.7 h before it reached STA although STA was located 0.04 AU sunward from the Earth.

Both at L1 and STA the magnetic field *N*-component changed from the north to the south indicating a bipolar (low inclination) ICME. At L1 the magnetic field points west at the center of the ICME while at STA the magnetic field fluctuates around the longitude 0°. We assign the flux rope category NWS for the ICME at L1 and the left-handed helicity. From the STA measurements we cannot determine the flux rope type or the helicity due to irregular magnetic field behavior.

The P_t profile at L1 shows a central maximum and the ICME thus belongs to Group 1. At STA the P_t profile does not stand out from the background because the magnetic field is not enhanced with respect to the ambient solar wind conditions within the ICME. This also makes the identification of the ICME boundaries more difficult, but in addition to the magnetic field rotation, the ICME interval at STA is featured by slightly depressed magnetic field fluctuation levels with respect to the background. As discussed above, the ICME appears less rope-like at STA than at L1 suggesting that STA traversed the ICME far from the center.

The suprathermal electron spectrograms show BDE intermittently during the ICME and after the ICME at L1, but at STA unidirectional heat flux is observed throughout the ICME. The ICME at STA was embedded in the away magnetic field sector. At L1 the magnetic field changed to the toward sector at the ICME leading edge and back to the away sector early 27 December. ICMEs at both spacecraft were surrounded by the slow speed solar wind and there was a region of enhanced solar wind density after their end boundary.

A possible CME source for the above described ICME was a faint and narrow CME that appeared in the field of view of the STB coronagraph around 15 UT on 19 December 2007. LASCO also observed this CME with the initial speed of 157 km/s at the position angle 319°, and the angular width of 43° as reported in the LASCO CME catalogue http://cdaw.gsfc.nasa.gov/CME_list/.

Based on the similar magnetic field behavior we conclude that STA and the L1 spacecraft encountered the same ICME. The P_t observations combined with more distinct ICME signatures at L1 than at STA suggest that the L1 spacecraft traversed the ICME close to the center while STA made only a glancing encounter through the ICME. Since this ICME had low inclination the spacecraft separation yields the lower limit for a half of the longitudinal extent of the ICME, about 20°.

3.2.4. Event 5: December 30, 2007–January 1, 2008

Between December 30, 2007–January 1, 2008 a particularly clear magnetic cloud was observed at STB (Fig. 6) that is included in the Kilpua et al. (2009a) list and in the UCLA ICME catalogue. In particular, the magnetic field signatures of this magnetic cloud were clear. The magnetic field direction rotated smoothly over a period of about two days. We searched ICME signatures from the L1 spacecraft that were located 22.8° away from STB and identified a region, where magnetic field rotation was very similar to that observed at STB. However, due to low magnetic field magnitude the rotation at L1 was not so pronounced as at STB. The leading edge of the ICME arrived at L1 about 16 h later than at STB although STB is located further from the Sun than the L1 spacecraft. The ICME was four times longer at STB than at L1 and the maximum magnetic field was also considerably higher at STB than at L1 (Table 1).

From Fig. 6 we see that at both spacecraft the magnetic field rotates from the north to the south while the magnetic field longitude angle remains directed to the west. Thus, we can identify this event as a bipolar ICME with the flux rope type NWS and left-handed helicity.

The P_t profile at STB shows a clear central maximum and the ICME is evidently crossed close to the center by STB. The flux rope signatures at L1 are very weak and also the P_t profile is irregular. The L1 spacecraft presumably made only a glancing encounter through the boundary of the ICME.

At both spacecraft the electron pitch angle spectrograms show unidirectional heat flux flow and the magnetic field is in the toward sector throughout the ICME. In the surrounding solar wind the magnetic field and the heat flux are in the opposite sector. At STB the polarity of the magnetic field changes at the leading edge of the ICME while at L1 the corresponding reversal occurred 10 h after the start of the ICME.

There is no doubt that STB crossed the ICME closer to the center than the L1 spacecraft. As it appears that STB traversed the flux rope close to the core and at L1 the flux rope was crossed close to its boundary, the separation between STB and the L1 spacecraft gives an estimate for the half width of the flux rope loop rather than for the total span. We conclude that this ICME likely spanned at least 40° in longitude.

3.2.5. Event 6: March 8–9, 2008

The left-side panels of Fig. 7 shows an ICME that was detected at L1 on 8–9 March 2008 embedded within a CIR. This ICME is included in the Kilpua et al. (2009a) list. The magnetic field within the ICME is substantially lower than in the surrounding solar wind, but a coherent magnetic field rotation is observed with the low variance of the magnetic field and depressed plasma beta. At STB no ICME signatures were identified, but STA detected a region with smoothly rotating magnetic field at the leading edge of a CIR. At STA a region of depressed temperature started well before the magnetic field rotation region, but it might be related to the slow speed solar wind. These events are discussed by Gomez-Herrero et al. (this issue) who studied the energetic particle acceleration associated with this interval.

The magnetic structure seems to be similar between L1 and STA. We see that magnetic field rotates from the north to the south (bipolar) through the time intervals indicated in Fig. 7. Magnetic field longitude angle points to the east and these ICMEs were assigned with the flux rope type NES and right-handed helicity.

Bidirectional electron intervals were not associated with either of the ICMEs. The ICME at STA carried a SBC from the toward to the away sector in the middle of the cloud, while at L1 the ICME was embedded in the away sector. Both events interacted strongly with the following high speed solar wind stream. Presumably due to this strong interaction with the ambient solar wind the P_t profiles are very irregular at both spacecraft.

As discussed by Gomez-Herrero et al. (this issue) STB observed two CME eruptions possibly connected with the observed ICMEs. The first CME that occurred near midday 4th March 2008 is a good candidate for producing the ICME at STA, while the timing considerations suggest that the latter CME that left early 5th March could be associated with the ICME at L1.

Although there are similarities in the magnetic structure of the ICMEs identified at L1 and STA it is possible that two different ICMEs were observed at these locations. The ICMEs were embedded within different solar wind sector structures and they both have

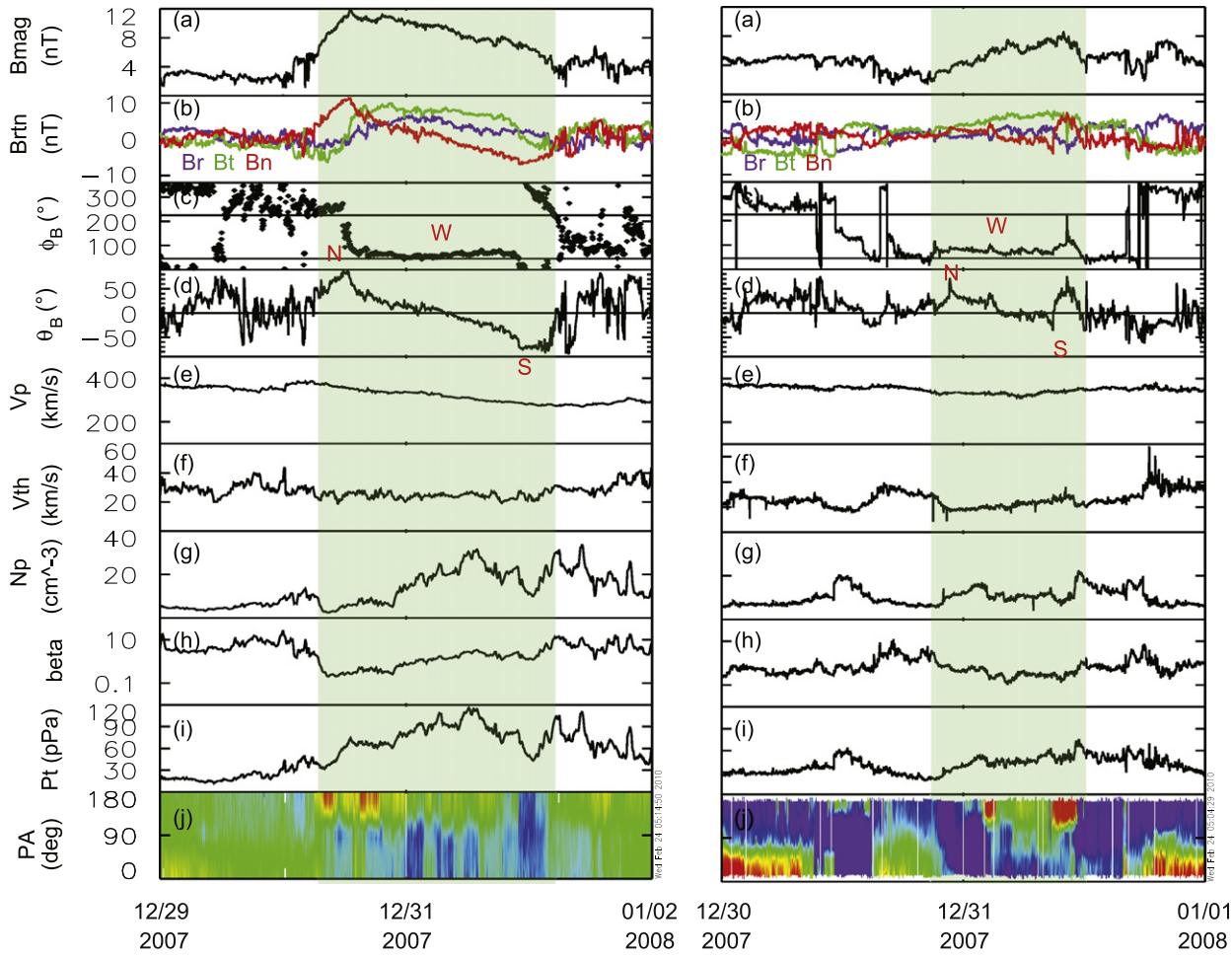

Fig. 6. Left: ICME observed at STB between 30 December 2007 0615 UT–1 January 2008 0230 UT. Right: ICME observed at Wind between 30 December 2150 UT–31 December 1135 UT. The panels are same as in Fig. 4.

separate CME candidates in a suitable time window. If both spacecraft detected the same ICME its angular span was at least $\sim 23^{\circ}$ (0.42 AU). Due to irregular P_t profiles it is hard to estimate the spacecraft crossing distances from the ICME center.

4. Discussion

ICMEs have been studied over several decades, but their three-dimensional structure remains yet unresolved. This is mainly due to the huge scale-sizes of ICMEs and the lack of systematic multi-spacecraft observations. In this paper we have reviewed the multi-point ICME observations before the STEREO mission and analyzed ICMEs that were detected by the L1 spacecraft and at least by one of the STEREO spacecraft during the one-year period from April 2007 to March 2008. We concentrated, in particular, on ICMEs that were identified by the spacecraft separated in longitude close to the ecliptic plane to exclude the possible latitudinal variations in the ICME structure. The radial separation between the STEREO and the L1 spacecraft is so small (STA are STB are separated by only ~ 0.08 AU in the radial direction) that no significant radial evolution should take place between the spacecraft.

Ten separate ICME events were reported for this one-year period in the ICME list in Kilpua et al. (2009a). From these 10 ICMEs we identified six events as possible multi-spacecraft encounters. The confident association between the ICME observations at different spacecraft becomes evidently difficult when the separation between the spacecraft increases. We do not expect that we would have identified more obvious multi-spacecraft ICME encounters if we had extended our survey to the end of 2008. At that time the separation between the STEREO spacecraft had reached almost 90°. In mid 2008 two very well-defined magnetic clouds with maximum magnetic fields of almost 15 nT were identified. The first one was observed at STA between 11–12 May 2008 and the latter at STB on 6–7 June 2008. We searched ICME signatures from Wind for both of these events, but did not find any indication of the ICME material. It is of course possible that the bulk of the CME plasma travelled west (east) of the STA (STB). As demonstrated by Jian et al. (2006, 2010) the solar minimum ICMEs are in general smaller and have lower magnetic fields than ICMEs at solar maximum. As a consequence they are less likely to be encountered by the spacecraft separated by several tens of degrees in longitude. Furthermore, weak ICMEs are difficult to observe from the ambient solar wind measurements.

Multipoint observations demonstrate that characteristics of identified ICMEs vary considerably from event to event. The reconstruction of the ICME structure for Events 1–2 by the Grad–Shafranov technique showed that the flux rope configuration seems to be a valid description at least in the core regions of some ICMEs (Liu et al., 2008; Möstl et al., 2009a,b). In addition, as indicated by the studies of Möstl et al. (2008, 2009b) the results from the optimized Grad–Shafranov method using multipoint ICME observations are essential for testing the assumptions of the technique, including the time-stationarity and translation symmetry along the invariant axis direction. Event 3 was clearly more complex and it could provide a fruitful event to test also the

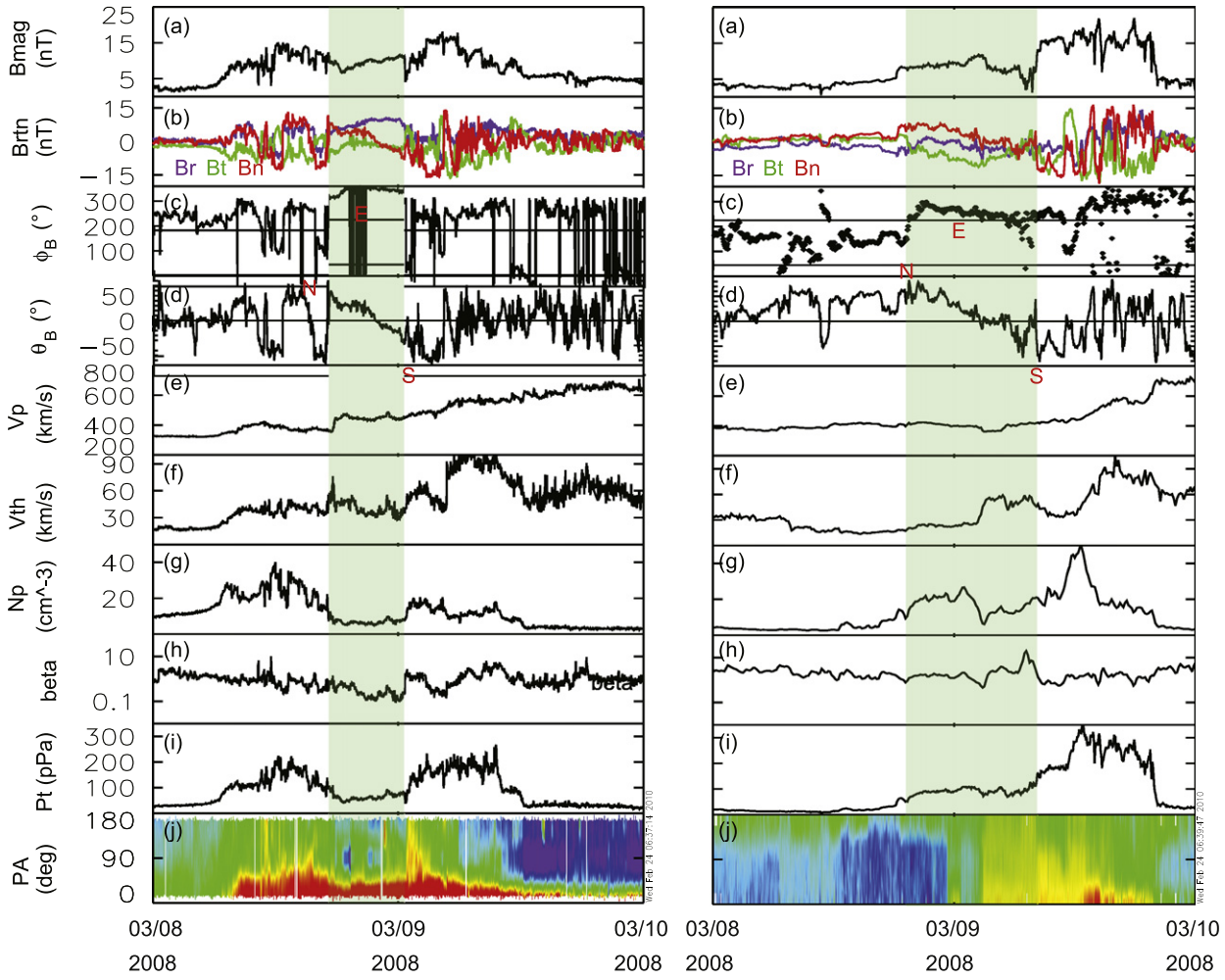

Fig. 7. Left: ICME observed at Wind between 8 March 1710 UT–9 March 0024 UT. Right: ICME observed at STA between 8 March 1820 UT–9 March 1040 UT. The panels are same as in Fig. 4.

spheroidal model. On the other hand, long-duration Event 5 could possibly feature a curved flux rope that was traversed twice through the axis (Rees and Forsyth, 2004; Marubashi and Lepping, 2007). For Events 3–6 the ICME leading edge arrived earlier at the spacecraft that was located further away from the Sun. This implies that the ICME leading edge structure is distorted or that the spacecraft traversed through different portions of the ICME (see also discussion about the global CME morphology for the 19–20 November event in Howard and Tappin, 2009).

As discussed in Section 2 the ICMEs identified by the spacecraft separated in latitude show highly oblate cross-sectional shapes with the aspect ratios approximately 1:6. However, cross-sectional shapes of high inclination ICMEs observed by the spacecraft separated in longitude range from nearly circular (Events 1–2 and Event M2) to significantly distended (Crooker and Intriligator, 1996). However, as discussed by Mulligan et al. (1999) one should be careful when interpreting the multi-spacecraft observations. The observations at Pioneer 11 and at the IMP spacecraft described in Crooker and Intriligator (1996) showed remarkably similar magnetic field signatures although the spacecraft were separated by about 30° in longitude. Thus, we believe that for this particular event the simple estimation of the ICME cross-section aspect ratio (1:8) reflects its true shape. The high inclination ICMEs studied by Mulligan et al. (1999) (Events M2 and M4) showed significantly more complex structure. Even for small spacecraft separation ($\sim$5°) there were clear differences in the rotation pattern of the magnetic field components. As the authors point out even though the spacecraft would encounter the same ICME it is possible that the ICME is highly distorted or the spacecraft traverses through different structures within the ICME. In addition, the authors also propose that some ICMEs might constitute from multiple interacting flux ropes that are ejected nearly simultaneously from the Sun. Such configurations would significantly complicate a simple analysis of the cross-sectional shape and the obtained aspect ratios should be considered only as rough estimations.

Möstl et al. (2009a) speculate that nearly circular cross-sections for the May 2007 magnetic clouds might result from the unusual ambient solar wind conditions as both magnetic clouds were running into a low solar wind pressure region ahead of a high speed stream. Riley et al. (2004) applied Grad–Shafranov method to two hypothetical time series derived from a global MHD simulation and showed that the Grad–Shafranov technique tends to underestimate the elongation of the ICME cross-section. As discussed in Kilpua et al. (2009a) for the first of the May 2007 magnetic clouds the GS reconstruction did not capture the whole interval of the magnetic field rotation associated with the ICME due to a shock within the ICME. If STA encountered the edge of the ICME that was observed at STB and at Wind (See Section 3.2.1), the observations indeed suggest that the cross-section was more stretched than deduced from the GS reconstruction. More extensive studies of magnetic cloud's cross-sectional shapes and how they are deformed by the solar wind interaction are needed in the future.

Besides the Grad–Shafranov reconstruction, also an elliptical model which includes the expansion of the cross-section has been used to study the distortion of magnetic clouds (Hidalgo, 2003; Riley and Crooker, 2004).

All the other ICMEs investigated in Section 3 except Events 1 and 2 had low inclinations. Thus, in these cases, the spacecraft separation gives a lower estimate of the longitudinal span of the flux rope loop. The last possible multi-spacecraft encounter during the investigated time interval occurred in March 2008 when the spacecraft (Wind and STA) were separated by 23°. If Event 3 was detected by all considered spacecraft, this ICME extended at least 40° in longitude. Also Event 5 presumably extended about 40° as well. These values are in agreement with the CME observations close to the Sun at solar minimum, when the average width of CMEs is about 47° (Yashiro et al., 2004). At solar maximum the average width of CMEs had increased to 61°, and thus it is expected that also ICMEs can have larger longitudinal widths at the years of high solar activity.

Although it is not surprising that low inclination ICMEs can span several tens of degrees in longitude near 1 AU, it is not evident that high inclination ICMEs can extent to such longitudinal distances. The multi-spacecraft observations have revealed that perpendicular ICMEs can extent at least up to 30° in longitude (ICME studied by Crooker and Intriligator, 1996 and Event M4). On the other hand, as discussed above, some perpendicular ICMEs may have almost circular cross-sections and clear differences are observed in their magnetic field structure even when the spacecraft are separated only few degrees in longitude. These observations suggest that, in general, high inclination ICMEs are more difficult to observe with the spacecraft widely separated in longitude than low inclination ICMEs.

It has been suggested by various authors that all ICMEs are ejected as flux ropes from the Sun, but in a majority of cases we fail to identify the flux rope structure in situ due to the large spacecraft crossing distances from the core of the ICME or due to the deformation of the initial flux rope structure as the ICME evolves on its way away from the Sun (e.g., Marubashi, 1997; Osherovich and Burlaga, 1997; Jian et al., 2006; Krall, 2007; Dasso et al., 2007). The multipoint observations of the ICME characteristics and their perpendicular pressure profiles conducted in this paper demonstrate that the flux rope signature disappears when the spacecraft crosses the ICME at large distances from the center. This result is consistent with the suggestion by Jian et al. (2006) that ICMEs at 1 AU have a central flux rope, but it is missed in a majority of cases. This assumption is now validated with the multi-spacecraft observations.

5. Conclusions

The multipoint ICME observations highlight that each ICME has its own complicated configuration. As a consequence ICMEs cannot be forced under a single simple model and one has to be careful when drawing conclusions from the multi-spacecraft observations. The chain of events that leads to the observed ICME near 1 AU includes complex processes in different plasma environments. The white-light CMEs close to the Sun as well as their source regions show large variety in their morphology. In addition, the erupting flux ropes can develop axial twist and rotation as they rise (Lynch et al., 2009) and each CME interacts with the unique solar wind structure. This poses a great challenge for the CME/ICME modellers. A better approximation is needed for the CME structure and the CMEs should be transported in the realistic solar wind structure away from the Sun (e.g., Odstrcil and Pizzo, 2009).

The confident association between the multipoint ICME observations becomes difficult when the separation between the spacecraft increases. Even at relatively small spacecraft separations significant differences can be identified in the magnetic field structure of ICMEs, in particular for high inclination ICMEs. The longitudinal span of low inclination ICMEs in the ecliptic plane seems to be consistent with the CME angular widths close to the Sun at solar minimum. The high inclination ICMEs exhibit plenty of variety in their cross-sectional shapes that is likely modified by the interaction with the ambient solar wind and the dynamics of the individual ICMEs. Multipoint ICME observations also demonstrate that the flux rope signature disappears when the spacecraft crossing distance from the ICME center increases.

Due to low solar activity only a few multi-spacecraft encounters have been identified using the combined observations of the STEREO and L1 spacecraft so far. Although STEREO spacecraft are now separating, more multipoint CME observations are expected when the spacecraft come close together at the far side of the Sun in 2014. According to the present solar cycle predictions this time period would coincide near solar maximum of cycle 24. In addition, in the declining phase the ICME rate should be considerably higher than at solar minimum as well as the ICMEs should have larger dimensions and stronger magnetic fields that will increase the probability of the multi-spacecraft encounters.

Acknowledgements

We thank R.P. Lin for the WIND 3D-plasma data, K.W. Ogilvie for the WIND SWE data and N. Ness for the ACE magnetic field data. We thank Adam Szabo for helping coordinate conversion of Wind magnetic field data. Support for the STEREO mission data processing and analysis was provided through NASA Contracts to the IMPACT, PLASTIC and SECCHI teams (the IMPACT contract to University of California Berkeley NAS5-03131, the PLASTIC Contract to University of New Hampshire NAS5-00132, and the SECCHI Contract to Naval Research Laboratory DPRS-13631-Y). STEREO suprathermal electron pitch angle distributions were achieved through the CESR SWEA server. We thank Andrea Opitz for validating the STEREO pitch angle distributions and Peter Schroeder and Davin Larson for compiling the Wind pitch angle distributions. The LASCO CME catalogue is generated and maintained at the CDAW Data Center by NASA and The Catholic University of America in cooperation with the Naval Research Laboratory. SOHO is a project of international cooperation between ESA and NASA. STEREO magnetic field and plasma data were achieved through UCLA Space Physics Center. Academy of Finland project 130298 is thanked for financial support.

References

Bothmer, V., Schwenn, R., 1998. The structure and origin of magnetic clouds in the solar wind. Annals of Geophysics 16, 1–24.

Burlaga, L., Sittler, E., Mariani, F., Schwenn, R., 1981. Magnetic loop behind an interplanetary shock: Voyager, Helios and IMP 8 observations. Journal of Geophysical Research 86, 6673–6684.

Burlaga, L., 1988. Magnetic clouds and force-free fields with constant alpha. Journal of Geophysical Research 93, 7217–7224.

Burlaga, L.F., Lepping, R.P., Jones, J.A., 1990. Global configuration of a magnetic cloud. In: Physics of Magnetic Flux Ropes. Geophysical Monograph, vol. 58. AGU, Washington, pp. 373–377.

Burlaga, L.F., Plunkett, S.P., St. Cyr, O.C., 2002. Successive CMEs and complex ejecta. Journal of Geophysical Research 107 (A10), 1266. doi:10.1029/2001JA000255.

Cid, C., Hidalgo, M.A., Nieves-Chinchilla, T., Sequeiros, J., Viñas, A.F., 2002. Plasma and magnetic field inside magnetic clouds: a global study. Solar Physics 207, 187–198.

Cremades, H., Bothmer, V., 2004. On the three-dimensional configuration of coronal mass ejections. Astronomy and Astrophysics 422, 307–322.

Crooker, N.U., Intriligator, D.S., 1996. A magnetic cloud as a distended flux rope occlusion in the heliospheric current sheet. Journal of Geophysical Research 101, 24,343–24,348.

Dasso, S., Mandrini, C.H., Démoulin, P., Luoni, M.L., Gulisano, A.M., 2005. Large scale MHD properties of interplanetary magnetic clouds. Advances in Space Research 35, 711–724.

Dasso, S., Nakwacki, M.S., Demoulin, P., Mandrini, C.H., 2007. Progressive transformation of a flux rope to an ICME. Solar Physics 244, 115–137.
Farrugia, C.J., Richardson, I.G., Burlaga, L.F., Lepping, R.P., Osherovich, V.A., 1993. Simultaneous observations of solar MeV particles in a magnetic cloud and in the earth's northern tail lobe—implications for the global field line topology of magnetic clouds and for the entry of solar particles into the magnetosphere during cloud passage. Journal of Geophysical Research 98, 15,497–15,507.
Farrugia, C.J., Osherovich, V.A., Burlaga, L.F., 1995. Magnetic flux rope versus the spheromak as models for interplanetary magnetic clouds. Journal of Geophysical Research 100 (A7), 12,293–12,306.
Farrugia, C.J., Janoo, L.A., Torbert, R.B., Quinn, J.M., Ogilvie, K.W., Lepping, R.P., Fitzenreiter, R.J., Steinberg, J.T., Lazarus, A.J., Lin, R.P., Larson, D., Dasso, S., Gratton, F.T., Lin, Y., Berdichevsky, D., 1999. A uniform-twist magnetic flux rope in the solar wind. In: Solar Wind Nine, AIP Conference Proceedings, vol. 471, American Institute of Physics, New York, pp. 745–748.
Foullon, C., Owen, C.J., Dasso, S., Green, L.M., Dandouras, I., Elliott, H.A., Fazakerley, A.N., Bogdanova, Y.V., Crooker, N.U., 2007. Multi-Spacecraft study of the 21 January 2005 ICME. Evidence of current sheet substructure near the periphery of a strongly expanding, fast magnetic cloud. Solar Physics 244, 139–165.
Goldstein, H., 1983. On the field configuration in magnetic clouds. In: Neugebauer, M., (Ed.), Solar Wind Five, Geophysics, NASA Conference Publications, pp. 731–733.
Gosling, J.T., 1990. Coronal mass ejections and magnetic flux ropes in interplanetary space. In: Priest, E.R., Lee, L.C., Russell, C.T. (Eds.), Physics of Magnetic Flux Ropes, Geophysical Monograph, vol. 58; 1990, pp. 343–364.
Gosling, J.T., 1997. Coronal mass ejections: an overview. In: Crooker, N., Joselyn, J.A., Feynman, J. (Eds.), Coronal Mass Ejections, Geophysical Monograph, vol. 99. AGU, pp. 9–16.
Gosling, J.T., Baker, D.N., Bame, S.J., Feldman, W.C., Zwickl, R.D., Smith, E.J., 1987. Bidirectional solar wind electron heatflux events. Journal of Geophysical Research 92 (A8), 8519–8535.
Gosling, J.T., McComas, D.J., Phillips, J.L., Bame, S.J., 1992. Counterstreaming solar wind halo electron events—solar cycle variations. Journal of Geophysical Research 97, 6351–6535. doi:10.1029/92JA00302.
Gosling, J.T., McComas, D.J., Phillips, J.L., Pizzo, V.J., Goldstein, B.E., Forsyth, R.J., Lepping, R.P., 1995. A CME-driven solar wind disturbance observed at both low and high heliographic latitudes. Geophysical Research Letters 22, 1753–1756.
Gosling, J.T., Riley, P., McComas, D.J., 1998. Overexpanding coronal mass ejections at high heliographic latitudes: observations and simulations. Journal of Geophysical Research 103, 1941–1954.
Gomez-Herrero, R., Malandraki, O., Dresing, N., Kilpua, E., Heber, B., Klassen, A., Muller-Mellin, R., Wimmer-Schweingruber, R.F. Multi-point observations of CIR-associated energetic particles during the 2008 solar minimum, this issue.
Gopalswamy, N., 2006. Coronal mass ejections of cycle 23. Journal of Astrophysics and Astronomy 27, 243–254.
Hidalgo, M.A., 2003. A study of the expansion and distortion of the cross section of magnetic clouds in the interplanetary medium. Journal of Geophysical Research 108 (A8). doi:10.1029/2002JA009818.
Hidalgo, M.A., Cid, C., Vinas, A.F., Sequeiros, J., 2002. A non-force-free approach to the topology of magnetic clouds in the solar wind. Journal of Geophysical Research 107 (A1). doi:10.1029/2001JA900100.
Howard, T.A., Tappin, S.J., 2009. Interplanetary coronal mass ejection observed in the heliosphere: 3. Physical implications. Space Science Reviews 147, 89–110.
Hu, Q., Sonnerup, B.U.O., 2002. Reconstruction of magnetic clouds in the solar wind: orientations and configurations. Journal of Geophysical Research 107 (A7). doi:10.1029/2001JA000293.
Huttunen, K.E.J., Schwenn, R., Bothmer, V., Koskinen, H.E.J., 2005. Properties and geoeffectiveness of magnetic clouds in the rising, maximum and early declining phases of solar cycle 23. Annales Geophysicae 23, 625–641.
Ivanov, K.G., Harshiladze, A.F., Eroshenko, E.G., Styazhkin, V.A., 1989. Configuration, structure, and dynamics of magnetic clouds from solar flares in light of measurements on board Vega 1 and Vega 2 in January–February 1986. Solar Physics 120, 407–419.
Jian, L., Russell, C.T., Luhmann, J.G., Skoug, R.M., 2006. Properties of interplanetary coronal mass ejections at one AU during 1995–2004. Solar Physics 239, 393–436.
Jian, L.K., Russell, C.T., Luhmann, J.G., Skoug, R.M., Steinberg, J.T., 2008a. Stream interactions and interplanetary coronal mass ejections at 0.72 AU. Solar Physics 249, 85–101.
Jian, L.K., Russell, C.T., Luhmann, J.G., Skoug, R.M., Steinberg, J.T., 2008b. Stream interactions and interplanetary coronal mass ejections at 5.3 AU, near the solar ecliptic plane. Solar Physics 250, 375–402.
Jian, L., Russell, C.T., Luhmann, J.G., Skoug, R.M., 2008c. Evolution of solar wind structures from 0.72 to 1 AU. Advances in Space Research 41, 259–266.
Jian, L.K., Russell, C.T., Luhmann, J.G., 2010. Comparing solar minimum 23/24 with historical solar wind records at 1 AU. Solar Physics, submitted.
Kaiser, M., Kucera, T.A., Davila, J.M., St. Cyr, O.C., Guhathakurta, M., Christian, E., 2007. The STEREO mission: an introduction, Space Science Reviews, doi:10.1007/s11214-007-9277-0.
Kilpua, E.K.J., Pomoell, J., Vourlidas, A., Vainio, R., Luhmann, J.G., Li, Y., Schroeder, P., Galvin, A.B., Simunac, K., 2009a. STEREO observations of interplanetary coronal mass ejections and prominence deflection during solar minimum period. Annales Geophysicae 27, 4401–4503.
Kilpua, E.K.J., Liewer, P.C., Farrugia, C., Luhmann, J.G., Möstl, C., Li, Y., Liu, Y., Lynch, B.J., Russell, C.T., Vourlidas, A., Acuna, M.H., Galvin, A.B., Larson, D., Sauvaud, J.A., 2009b. Multispacecraft observations of magnetic clouds and their solar origins between 19 and 23 May 2007. Solar Physics 254, 325–344.
Krall, J., 2007. Are all coronal mass ejections hollow flux ropes? The Astrophysical Journal 657, 559–566.
Lepping, R.P., Jones, J.A., Burlaga, L.F., 1990. Magnetic field structure of interplanetary magnetic clouds at 1 AU. Journal of Geophysical Research 95, 11,957–11,965.
Lepping, R.P., Berdichevsky, D.B., Wu, C.-C., Szabo, A., Narock, T., Mariani, F., Lazarus, A.J., Quivers, A.J., 2006. A summary of WIND magnetic clouds for years 1995–2003: model-fitted parameters, associated errors and classifications. 24, 215–245.
Li, Y., Luhmann, J.G., 2004. Solar cycle control of the magnetic cloud polarity and the geoeffectiveness. Journal of Atmospheric and Solar-Terrestrial Physics 66, 323–331.
Liu, Y., Richardson, J.D., Belcher, J.W., 2005. A statistical study of the properties of interplanetary coronal mass ejections from 0.3 to 504 AU. Planetary and Space Science 53 (1–3), 3–17.
Liu, Y., Richardson, J.D., Belcher, J.W., Wang, C., Hu, Q., Kasper, J.C., 2006. Constraints on the global structure of magnetic clouds: transverse size and curvature. Journal of Geophysical Research 111. doi:10.1029/2006JA011890.
Liu, Y., Luhmann, J.G., Huttunen, K.E.J., Lin, R.B., Bale, S.D., Russell, C.T., Galvin, A.B., 2008. Reconstruction of the 2007 May 22 magnetic cloud: how much can we trust the flux-rope geometry of CMEs? Astrophysical Journal Letters 677, L133–L136.
Lundquist, S., 1950. Magnetohydrostatic fields. Arkiv foer Fysik 2, 361–365.
Lynch, B.J., Antiochos, S.K., Li, Y., Luhmann, J.G., DeVore, C.R., 2009. Rotation of coronal mass ejections during eruption. Astrophysical Journal 2, 1918–1927.
Maia, D., Aulanier, G., Wand, S.J., Pick, M., Malherbe, J.-M., Delaboudiniere, J.-P., 2003. Interpretation of a complex CME event: coupling of scales in multiple flux systems. Astronomy and Astrophysics 405, 313–323.
Malandraki, O., Saris, E.T., Kasotakis, Gr., Sidiropoulos, N., 2000. Study of CME structure and evolution deduced from Ulysses/Hi-scale energetic particle observations. Advances Space Research 26, 875–878.
Manchester, W.B., Gombosi, T.I., Roussev, I., Ridley, A., De Zeeuw, D.L., Sokolov, I.V., Powell, K.G., Toth, G., 2004. Modeling a space weather event from the Sun to the Earth: CME generation and interplanetary propagation. Journal of Geophysical Research 109 (A2). doi:10.1029/2003JA010150.
Manchester, W.B., Zurbuchen, T.H., 2007. Reply to comment by P. Riley and J.T. Gosling on "Are high-latitude forward-reverse shock pairs driven by overexpansion?", Journal Geophysical Research, 112 (A7), doi:10.1029/2007JA012272.
Marubashi, K., 1986. Structure of the interplanetary magnetic clouds and their solar origins. Advances Space Research 6, 335–338.
Marubashi, K., 1997. Interplanetary magnetic flux ropes and solar filaments. In: Crooker, N., Joselyn, J.A., Feynmann, J. (Eds.), Coronal Mass Ejections, Geophysical Monograph Series, vol. 99. AGU, Washington, DC, pp. 147–156.
Marubashi, K., Lepping, R.P., 2007. Long-duration magnetic clouds: a comparison of analyses using torus- and cylinder-shaper flux rope models. Annales Geophysicae 25, 2453–2477.
Möstl, C., Miklenic, C., Farrugia, C.J., Temmer, M., Veronig, A., Galvin, A.B., Vrsnak, B., Biernat, H.K., 2008. Two-spacecraft reconstruction of a magnetic cloud and comparison to its solar source. Annales Geophysicae 26, 3139–3152.
Möstl, C., Farrugia, C.J., Miklenic, C., Temmer, M., Galvin, A.B., Luhmann, J.G., Kilpua, E.K.J., Leitner, M., Nieves-Chinchilla, T., Veronig, A., Biernat, H.K., 2009a. Multi-spacecraft recovery of a magnetic cloud and its origin from magnetic reconnection on the Sun. Journal of Geophysical Research 114 (A4). doi:10.1029/2008JA013657.
Möstl, C., Farrugia, C.J., Biernat, H.K., Leitner, M., Kilpua, E.K.J., Galvin, A.B., Luhmann, J.G., 2009b. Optimized Grad–Shafranov reconstruction of a magnetic cloud using STEREO-wind observations. Solar Physics 256, 427–441.
Mulligan, T., Russell, C.T., Luhmann, J.G., 1998. Solar cycle evolution of the structure of magnetic clouds in the inner heliosphere. Geophysical Research Letters 25, 2959–2962.
Mulligan, T., Russell, C.T., Anderson, B.J., Lohr, D.A., Rust, D., Toth, B.A., Zanetti, L.J., Acuna, M.H., Lepping, R.P., Golsing, J.T., 1999. Intercomparison of NEAR and Wind interplanetary coronal mass ejection observations. Journal of Geophysical Research 104, 28,217.
Mulligan, T., Russell, C.T., 2001. Multispacecraft modeling of the flux rope structure of interplanetary coronal mass ejections: cylindrically symmetric versus non-symmetric topologies. Journal of Geophysical Research 106, 10,581–10,596.
Neugebauer, M., Goldstein, R., 1997. Particle and field signatures of coronal mass ejections in the solar wind. In: Crooker, N., Joselyn, J.A., Feynman, J. (Eds.), Coronal Mass Ejections, Geophysical Monograph, vol. 99. AGU, pp. 245–252.
Odstrcil, D., Pizzo, V.J., 2009. Numerical heliospheric simulations as assisting tool for interpretation of observations by STEREO heliospheric imagers. Solar Physics 259, 297–309.
Osherovich, V., Burlaga, L.F., 1997. Magnetic clouds. In: Crooker, N., Joselyn, J.A., Feynmann, J. (Eds.), Coronal Mass Ejections, Geophysical Monograph Series, vol. 99. AGU, Washington, DC, pp. 157–158.
Owens, M.J., Merkin, V.G., Riley, P., 2006. A kinematically distorted flux rope model for magnetic clouds. Journal of Geophysical Research 111 (A3). doi:10.1029/2005JA011460.
Paularena, K.I., Wang, C., von Steiger, R., Heber, 2001. B., An ICME observed by voyager 2 at 58 AU and by Ulysses at 5 AU, Geophysical Research Letters 28, 2755–2758.
Rees, A., Forsyth, R.J., 2004. Two examples of magnetic clouds with double rotations observed by the Ulysses spacecraft. Geophysical Research Letters 31, L06804. doi:10.1029/2003GL018330.

Reisenfeld, D.B., Gosling, J.T., Forsyth, R.J., Riley, P., St. Cyr, O.C., 2003. Properties of high-latitude CME-driven disturbances during Ulysses second northern polar passage. Geophysical Research Letters 30. doi:10.1029/2003GL017155.

Richardson, I.G., Cliver, E.W., Cane, H.V., 2001. Sources of geomagnetic storms for solar minimum and maximum conditions during 1972–2000. Journal of Geophysical Research 28, 2569.

Richardson, I.G., Cane, H.V., 2004a. Identification of interplanetary coronal mass ejections at 1 AU using multiple solar wind plasma composition anomalies. Journal of Geophysical Research 109, A09104. doi:10.1029/2004JA010598.

Richardson, I.G., Cane, H.V., 2004b. The fraction of interplanetary coronal mass ejections that are magnetic clouds: evidence for a solar cycle variation. Geophysical Research Letters 31, L18804. doi:10.1029/2004GL020958.

Richardson, J.D., Liu, Y., Wang, C., Burlaga, L.F., 2006. ICMEs at very large distances. Advances in Space Research 3, 528–534.

Riley, P., Linker, J.A., Mikic, Z., Odstrcil, D., Zurbuchen, T.H., Lario, D., Lepping, R.P., 2003. Using an MHD simulation to interpret the global context of a coronal mass ejection observed by two spacecraft. Journal of Geophysical Research 108 (A7). doi:10.1029/2002JA009760.

Riley, P., Crooker, N.U., 2004. Kinematic treatment of coronal mass ejection evolution in the solar wind. The Astronomical Journal 600, 1035–1042.

Riley, P., Linker, J.A., Lionello, R., Mikic, Z., Odstrcil, D., Hidalgo, M.A., Cid, C., Hud, Q., Lepping, R.P., Lynch, B.J., Rees, A., 2004. Fitting flux ropes to a global MHD solution: a comparison of techniques. 66, 1321–1331.

Riley, P., Schatzman, C., Cane, H.V., Richardson, I.G., Gopalswamy, N., 2006. On the rates of coronal mass ejections: remote solar and in situ observations. The Astrophysical Journal 647, 648–653.

Russell, C.T., Mulligan, T., 2002. The true dimensions of the interplanetary coronal mass ejections. Advances in Space Research 29, 306–310.

Russell, C.T., Shinde, A.A., Jian, L., 2005. A new parameter to define interplanetary coronal mass ejections. Advances in Space Research 12, 2178–2184.

Steinberg, J.T., Gosling, J.T., Skoug, R.M., Wiend, R.C., 2005. Suprathermal electrons in high-speed streams from coronal holes: counterstreaming on open field lines at 1 AU. Journal of Geophysical Research 110, A06103. doi:10.1029/2005JA011027.

St. Cyr, O.C., Howard, R.A., Sheeley, N.R., Plunkett, S.P., Michels, D.J., Paswaters, S.E., Koomen, M.J., Simnett, G.M., Thomson, B.J., Gurman, J.B., Schwenn, R., Webb, D.F., Hildner, E., Lamy, P.L., 2000. Properties of coronal mass ejections: SOHO LASCO observations from January 1996 to June 1998. Journal of Geophysical Research 105 (A8). doi:10.1029/1999JA000381.

Vandas, M., Fischer, S., Pelant, P., Geranios, A., 1993a. Spheroidal models of magnetic clouds and their comparison with spacecraft measurements. Journal of Geophysical Research 98 (A7), 11,467–11,475.

Vandas, M., Fischer, S., Pelant, P., Geranios, A., 1993b. Evidence for a spheroidal structure of magnetic clouds. Journal of Geophysical Research 98 (A12), 21,061–21,069.

Vandas, M., Romashets, E., Watari, S., 2005. Magnetic clouds of oblate shapes. Planetary and Space Science 53, 19–24.

von Steiger, R., Richardson, J.D., 2006. ICMEs in the outer heliosphere and high latitudes: an introduction. Advances in Space Research 123, 111–126.

Vourlidas, A., Howard, R.A., 2006. The proper treatment of coronal mass ejection brightness: a new methodology and implications for observations. The Astrophysical Journal 642, 1216–1221.

Wang, C., Richardson, J.D., 2004. Interplanetary coronal mass ejections observed by Voyager 2 between 1 and 30 AU. Journal of Geophysical Research 106, 5683–5692. doi:10.1029/2004JA010379.

Webb, D.F., Cliver, E.W., Crooker, N.U., St Cry, O.C., Thomson, B.J., 2000. Relationship of halo coronal mass ejections, magnetic clouds, and magnetic storms. Journal of Geophysical Research 105, 7491–7508.

Yashiro, S., Gopalswamy, N., Michalek, G., St Cyr, O.C., Plunkett, S.P., Rich, N.B., Howard, R.A., 2004. A catalog of white light coronal mass ejections observed by the SOHO spacecraft. Journal of Geophysical Research 109 (A7). doi:10.1029/2003JA010282.

Zurbuchen, T.H., Richardson, I.G., 2006. In-situ solar wind and magnetic field signatures of interplanetary coronal mass ejections. Space Science Reviews 123, 1572.